Widely Wavelength-Tunable Ultrashort Pulse Generation Using Polarization Maintaining Optical Fibers

Norihiko Nishizawa, *Member, IEEE,* and Toshio Goto, *Senior Member, IEEE*

***Abstract*—Characteristics of widely wavelength tunable ultrashort pulse generation using several types of polarization maintaining fibers have been experimentally analyzed. Using the diameter reduced type of polarization maintaining fibers, the wavelength tunable soliton pulse is generated from 1.56 to 2.03 μm. It is confirmed that the almost transform-limited 340-fs soliton pulse is generated at a wavelength of around 2 μm using a frequency-resolved optical gating method. When the low-birefringent fibers are used, it is observed that the orthogonally polarized small pulse spectrum is trapped by the soliton pulse and is also shifted toward the longer wavelength side in the process of soliton self-frequency shift. The wavelength of the orthogonally polarized pulse spectrum is 40–50 nm longer than that of the soliton pulse, and the birefringence of the fiber is compensated by the chromatic dispersion. Finally, the polarization maintaining highly nonlinear dispersion-shifted fiber is used as the sample fiber. When the fiber input power is low, the wavelength-tunable soliton and anti-stokes pulses are generated. As the fiber input power is increased, the pulse spectra are gradually overlapped and the 1.1–2.1 μm widely broadened supercontinuum spectra are generated by only 520 pJ pulse energy.**

***Index Terms*—Nonlinear wave propagation, optical fiber applications, optical fiber lasers, optical pulse generation, optical soliton, Raman scattering.**

I. Introduction

ULTRASHORT pulse lasers are an important light source for ultrafast optoelectronics, ultrafast spectroscopy, multiphoton microscopy, optical chemistry, etc. So far, as ultrashort pulse lasers, the large scaled dye laser or solid-state laser have been used. However, the size of those systems is not compact, and they have been difficult to handle. In addition, the practical wavelength-tunable ultrashort pulse source at a wavelength above 1 μm has not been demonstrated.

Recently, the passively mode-locked fiber laser has been demonstrated by several groups [1]–[6]. These lasers are compact and stable and almost maintenance-free. However, the wavelengths of the optical pulses are fixed around 1.55 μm and cannot be changed widely.

Recently, we have succeeded in the demonstration of a wavelength-tunable compact system for short pulse generation with the combination of a fiber laser and an optical fiber [7]–[10]. In this system, the wavelength of the soliton pulse can be changed continuously by merely varying the fiber input power. In the first paper, the wavelength of the soliton pulse has been changed at the wavelength region of 1.56–1.78 μm [7]. The generated pulses are estimated as 200 fs by the assumption of sech^2 pulse shape, and they are close to the ideal soliton pulses from the time-bandwidth product. The maximum conversion efficiency from the pump pulse into the soliton pulse is as high as 85%. Then the two colored soliton pulses have been generated simultaneously using the birefringence of the polarization maintaining (PM) fibers [8]. Using the dispersion-shifted fibers, we can generate the wavelength-tunable soliton pulse and the anti-stokes pulse in the wavelength region of 1.32–1.75 μm [10]. This wavelength conversion technique has been used in the high-power fiber laser systems [11]. Recently, the electrically controlled high-speed wavelength-tunable ultrashort pulse generation has been demonstrated using the acoustooptical modulator and optical fibers [12].

In this paper, the wavelength-tunable ultrashort pulse generation is examined and characterized using several types of PM fibers. Widely wavelength-tunable ultrashort soliton pulse is generated in the wavelength region of 1.55–2.03 μm. The generated soliton pulse around 2.0 μm is observed using the technique of frequency-resolved optical gating (FROG). Then, the observed phenomenon of spectral trapping between the orthogonal polarization components in the low birefringent PM fibers is discussed. Finally, the characteristics of the spectral variation in PM highly nonlinear dispersion-shifted fibers are experimentally investigated. The widely broadened supercontinuum generation is observed in the wavelength region of 1.1–2.1 μm.

II. Widely Wavelength- Tunable Soliton Pulse Generation Using Diameter Reduced Fiber

Fig. 1 shows the experimental setup. The passively mode-locked Er-doped fiber laser (IMRA Femtolight) is used as the light source. It generates the 110 fs sech^2-like pulses stably at a repetition rate of 48 MHz. The center wavelength is 1556 nm and the spectral width is about 20 nm. The output of the fiber laser is coupled into the optical fibers. In this section, the diameter reduced type of PM fibers are used as the wavelength conversion fibers. The mode field diameter is 5.8 μm, and the magnitude of the dispersion $\beta_2 = -15$ ps^2/km at the wavelength of 1.55 μm. The polarization direction of the pump pulse is aligned along the birefringent axis of the fiber. In the optical fibers, the pulse breakup occurs in the ultrashort pulse propagation and the wavelength tunable soliton pulses are generated due to the soliton self-frequency shift [7], [13]–[16]. As the

Manuscript received January 4, 2001; revised June 18, 2001.

The authors are with the Department of Quantum Engineering, Nagoya University, Nagoya 464-8603, Japan.

Publisher Item Identifier S 1077-260X(01)09947-6.

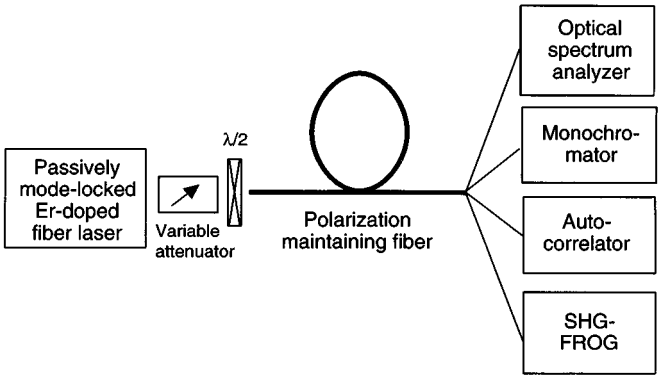

Fig. 1. Experimental setup of widely wavelength-tunable ultrashort pulse generation.

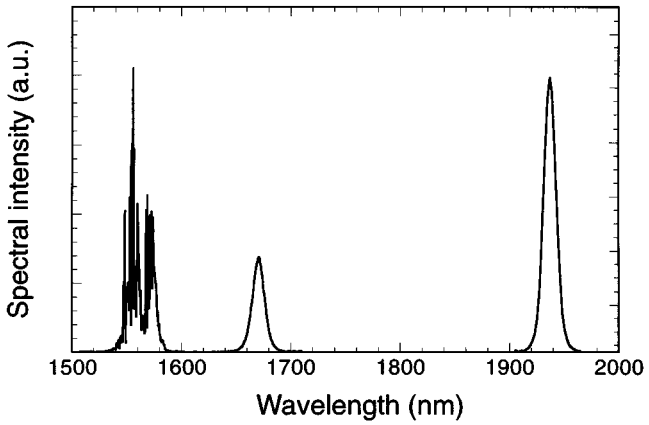

Fig. 2. Observed optical spectra at the fiber output when diameter reduced type PM fiber is used. The fiber input power is 30 mW and the fiber length is 220 m.

fiber input power varies, the wavelength of the generated soliton pulse is shifted arbitrarily and continuously.

Fig. 2 shows the observed optical spectra at the output of the 220-m PM fibers when the fiber input power is 30 mW. The optical spectra are measured with the optical spectrum analyzer and the monochromator. When the fiber input power is increased, the wavelength of the soliton pulse is shifted toward the longer wavelength side. The observed maximum conversion efficiency from the pump pulse into the soliton pulse is as high as 85% when the fiber length is 75 m, fiber input power is 5.5 mW, and center wavelength of the soliton is 1625 nm. As the fiber input power is much increased, following the first solitons, the second soliton pulse is generated from the residual pump pulse, which is not converted into the soliton pulse. The generated soliton pulses are almost the transform-limited ideal sech^2 pulses. When the conventional non-PM fibers are used, the clear sech^2 pulses are not generated.

In [17], we have experimentally analyzed the wavelength dependence for conversion efficiency [17]. In that study, the magnitude of the conversion efficiency is gradually decreased as the wavelength shift of the soliton pulse is increased due to the increasement of the absorption loss in the optical fiber. As the results of the numerical analysis, almost perfect conversion efficiency has been obtained when the input pulse is the fundamental soliton pulse [9].

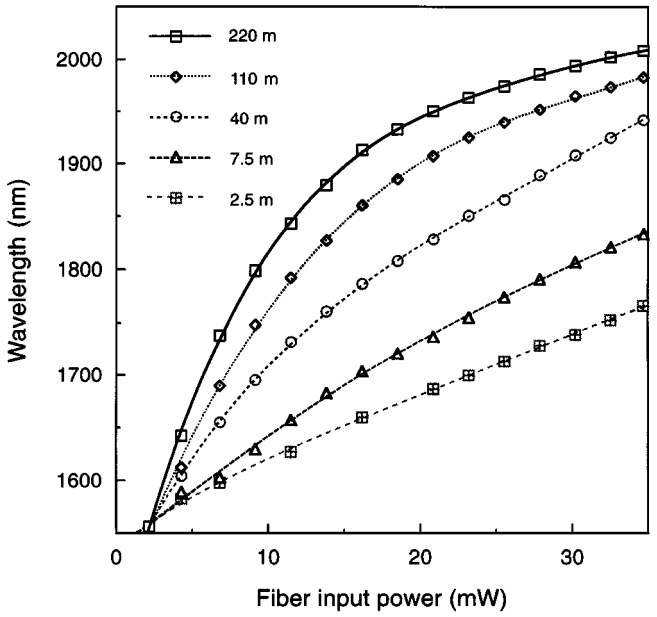

Fig. 3. Characteristics of wavelength shift of soliton pulse as the function of fiber input power when the diameter reduced type PM fiber is used.

Fig. 3 shows the characteristics of the wavelength shift of the first soliton pulse as a function of the fiber input power. As the fiber input power is increased, the wavelength of the generated soliton pulse is shifted continuously toward the longer wavelength side. For the wavelength region of 1.55–1.85 μm, the wavelength of the soliton pulse is shifted almost linearly and continuously as a function of the fiber input power. In terms of the fiber length, the longer the fiber is, the larger the wavelength of the soliton pulse is. When the fiber length is 220 m and the fiber input power is 35 mW, the wavelength of the soliton pulse is shifted up to 2008 nm. When the fiber input power is much increased to 45 mW, the maximum wavelength shift up to 2033 nm is observed. The magnitude of wavelength shift is as large as 475 nm.

Above the wavelength of 1.85 μm, the slope of the wavelength shift is gradually decreased. This decrease of the slope of wavelength shift is due to the increase of mode-field radius, magnitude of chromatic dispersion, and optical attenuation loss as the wavelength of the soliton pulse is increased [9].

The observed autocorrelation trace of the soliton pulse is shown in Fig. 4. The fiber length is 110 m and the fiber input power is 7 mW. The pedestal free clear trace is observed, and this autocorrelation trace is well fitted to that of the sech^2 pulse. The temporal width of the autocorrelation trace is 330 fs at full-width at half-maximum (FWHM) and the corresponding pulse width is estimated to be 210 fs. The time–bandwidth product is 0.32 and is in good agreement with that of the transform limited sech^2 pulse. The soliton number N is estimated to be $\sim$1 and the ideal soliton pulse is generated.

In this system, the observed maximum wavelength of the soliton pulse reached up to 2.03 μm. It is, however, difficult to measure the actual temporal width since the second soliton pulse and the residual pump pulse come out together with the first generated soliton pulse. In this paper, we observe the soliton pulse

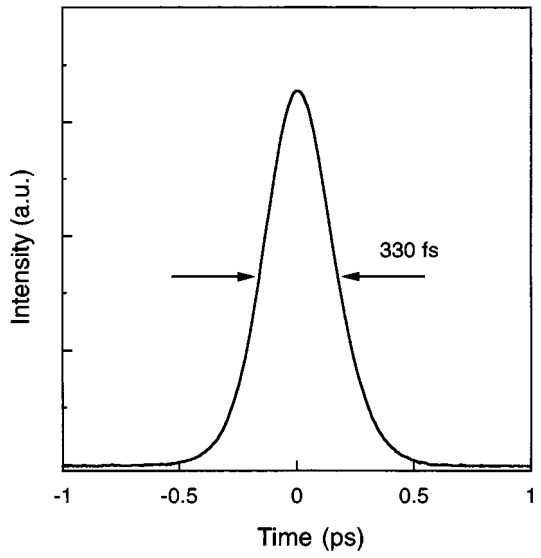

Fig. 4. Observed autocorrelation trace of soliton pulse when the diameter reduced type PM fiber is used. The fiber length is 110 m and the fiber input power is 7 mW.

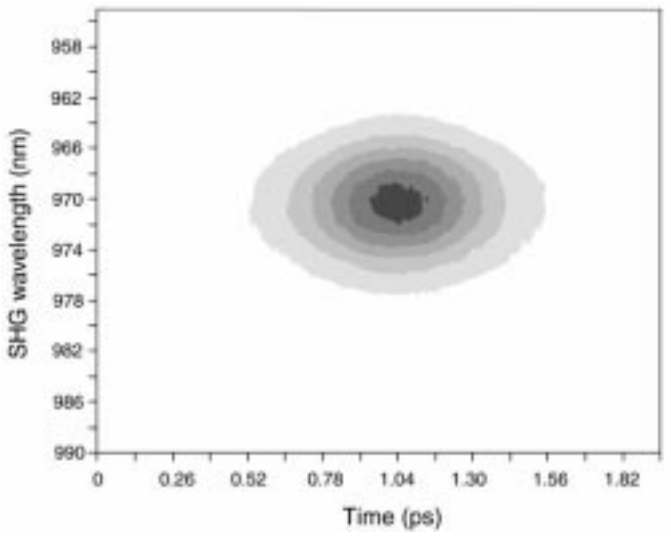

Fig. 5. Observed SHG-FROG trace of wavelength-tunable soliton pulse around 2 μm when the diameter reduced PM fiber is used. The fiber length is 220 m and the fiber input power is 30 mW.

using the second harmonic generation (SHG) FROG method, and the temporal width of the soliton pulse has been estimated.

Fig. 5 shows the measured FROG trace of the generated soliton pulse at the wavelength of 1942 nm. The fiber length is 220 m and the fiber input power is 30 mW, which is almost the same condition as in Fig. 2. The 3-mm-thick KTP crystal is used as the SHG crystal to generate the correlation signals [18]. The generated SHG signals are passed through the monochromator and detected with the photomultiplier. In Fig. 5, the elliptical symmetric trace is clearly observed. The temporal width of the autocorrelation trace obtained from the FROG trace is 520 fs at FWHM and the corresponding pulse width is 340 fs under the assumption of the sech^2 pulse shape. From Fig. 2, the spectral width is 13 nm and the corresponding time bandwidth product is 0.35. This value is slightly larger than that of the transform-limited sech^2 pulse, which is 0.315. From this figure, it is confirmed that the nearly transform-limited femtosecond soliton pulse is generated at a wavelength of around 2 μm.

The characteristics of ultrashort pulse propagation in optical fibers can be described by the nonlinear Schrödinger equation [19]. The results of numerical analysis are well in agreement with the experimental ones [9]. The maximum wavelength shift has been estimated to be 2.2 μm by the numerical simulation. In the experiment, the observed maximum wavelength of the Raman-shifted soliton pulse is 2130 nm [6]. It is considered that if we can use the intense and ideal pump pulse, we can obtain the much larger wavelength shift experimentally.

In [20], we have experimentally observed the magnitude of timing jitter of the wavelength-tunable soliton pulse in the wavelength region of 1600–1700 nm [20]. It has been shown that the magnitude of the timing jitter is not increased as much in the process of soliton self-frequency shift. Thus it can be said that this wavelength-tunable ultrashort pulse generation system is very stable, and it is very useful for practical applications.

Since the wavelength shift of the soliton pulse is induced by the nonlinear effect in the optical fibers, the wavelength can be varied very rapidly using the intensity modulator. Recently, the ultra-high-speed wavelength-tunable ultrashort pulse generation system has been demonstrated using the acoustooptical modulator [12].

III. Orthogonal Spectral Trapping in Low Birefringent Fiber

In the previous section, we have used the diameter reduced type of PM fiber in which the magnitude of mode field diameter is 5.8 μm and the typical birefringence is about 7×10^{-4}. A decade years ago, Islam *et al.* observed the soliton trapping between the two orthogonal polarization components using very low birefringent fiber, in which the magnitude of birefringence is about 2×10^{-5} [21]. In this section, we describe the experimental results of the low-birefringent fiber, in which the magnitude of mode-field diameter is 8 μm and the typical birefringence is 3×10^{-4}.

Fig. 6 shows the observed optical spectra at the fiber output. The fiber length is 220 m and the fiber input power is 24 mW. When the polarization direction is aligned along the fast axis of the PM fiber, the monocolored soliton pulse is generated at the longer wavelength side of the pump pulse. This soliton pulse is almost the transform-limited fundamental soliton pulse [17]. When the polarization direction is aligned along the slow axis, in addition to the generated soliton pulse, the small pulse spectral component is observed at the 40 nm longer wavelength side of the soliton pulse.

Fig. 6(c) and (d) shows the observed optical spectra when the polarizer is used to pick up one of the orthogonal polarization components. The polarization direction of the fiber input pulse is aligned along the slow axis of the PM fiber. When the polarizer at the fiber output is adjusted to pick up the slow axis components, the soliton pulse and the residual pump pulse, which is not converted into the soliton pulse, are observed. On the other hand, when the polarizer is adjusted to pick up the fast axis components, the spectral component of the soliton pulse is almost removed and the small pulse component at the longer wavelength

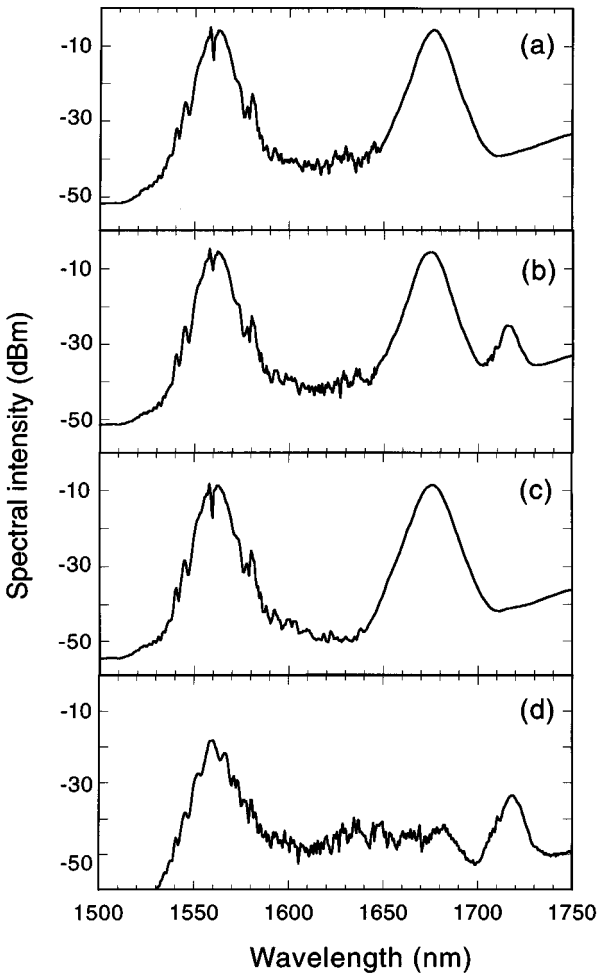

Fig. 6. Observed optical spectra at the fiber output when the low birefringent fiber is used. The fiber input power is 24 mW and the fiber length is 220 m. The polarization direction of the fiber input pulse is aligned along (a) the fast axis and (b)–(d) the slow axis. (a) and (b) are the spectra at fiber output, (c) is that of slow axis components, and (d) is that of fast axis components.

side of the soliton pulse and the residual pump pulse are clearly observed. Thus it is clarified that the polarization direction of the soliton pulse is orthogonal to that of the small pulse spectra at the longer wavelength side of the pump pulse.

Fig. 7 shows the characteristics of the wavelength shift of generated soliton pulse and small pulse spectra. The wavelength of the soliton pulse is shifted almost linearly above the threshold power as the fiber input power is changed. For the same input power, the center wavelength of the soliton pulse that is aligned along the fast axis is equal to that aligned along the slow axis. When the polarization direction of the soliton pulse is aligned along the slow axis, the small pulse spectrum is generated at the 40–50 nm longer wavelength side of the soliton pulse. When the wavelength of the soliton pulse is shifted toward the longer wavelength side by the soliton self-frequency shift, this small spectral part is also shifted toward the longer wavelength side, keeping the wavelength separation from the soliton pulse. It looks like the trapping of the small spectrum by the soliton pulse.

Owing to the birefringence of the optical fiber, the slow axis component propagates slower than the fast axis component

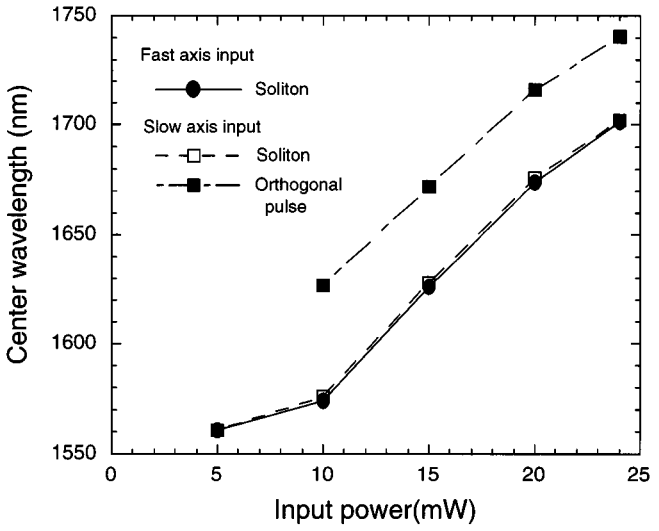

Fig. 7. Characteristics of wavelength shifts of soliton and orthogonally polarized small pulse spectra when the low birefringent fiber is used. The fiber length is 220 m.

when the optical wavelength is fixed. The magnitude of the birefringence is about 3×10^{-4} and the magnitude of the time delay is estimated to be 1 ps/m.

Since the wavelength of the small spectral component is longer than that of the soliton pulse, the small spectral part propagates slower than the soliton pulse owing to the chromatic dispersion when the polarization state is in the same condition. In Fig. 7, when the fiber output power is 10 mW, the wavelengths of the soliton pulse and the small pulse spectrum are 1574 and 1627 nm, respectively, and the magnitude of the wavelength separation is 53 nm. In this wavelength, the magnitude of β_2 is estimated to be about -30 ps^2/km. Thus the delay time that is induced by the wavelength separation is estimated to be 1.3 ps/m. When the fiber output power is 24 mW, the wavelengths of the soliton pulse and the small pulse spectrum are 1701 and 1740 nm, respectively. The magnitude of the wavelength separation is 39 nm and is slightly decreased from that mentioned above. In this wavelength, the magnitude of β_2 is estimated to be about -45 ps^2/km, and the delay time due to the wavelength separation is estimated to be 1.4 ps/m.

From the above estimations, we can see that the magnitudes of the delay times induced by the chromatic dispersion are almost equal to that induced by the birefringence. Thus it can be considered that the effect of the birefringence is compensated by the chromatic dispersion, and the soliton pulse and the small spectral component copropagate along the fiber. As the wavelength shift of the soliton pulse is advanced and the magnitude of the chromatic dispersion is increased, the magnitude of the wavelength separation between the soliton pulse and the small spectrum is gradually decreased and the propagation velocities of the two pulses are kept equal. We can consider as this phenomenon that the small spectral component is trapped by the soliton pulse.

The delay time induced by the chromatic dispersion is slightly larger than that induced by the birefringence. The reason considered is that the wavelengths of the soliton pulse and the small pulse spectrum gradually increase as the pulse propagation.

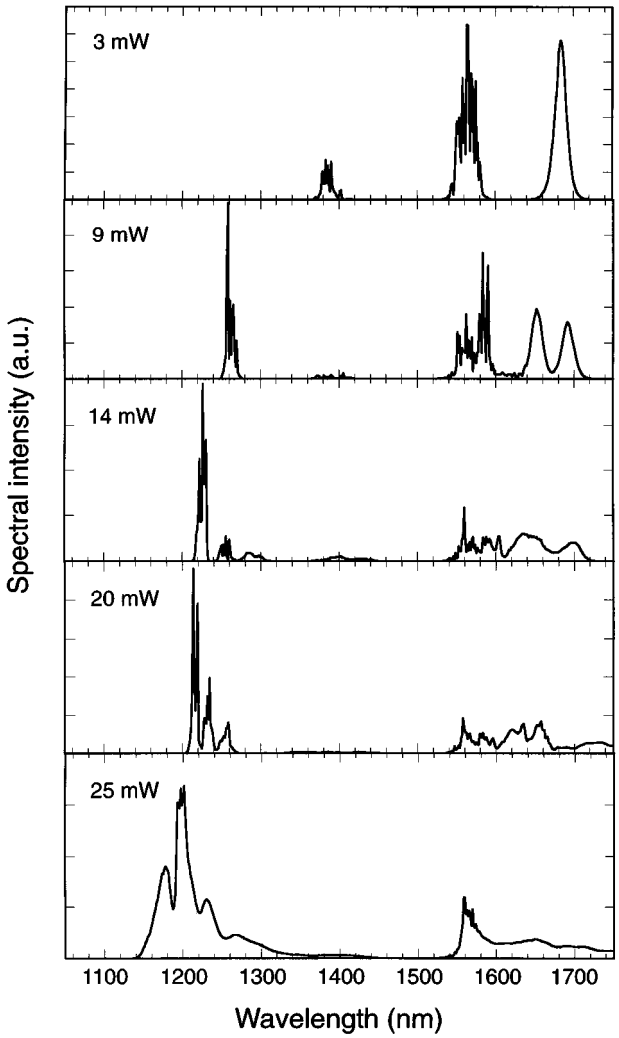

Fig. 8. Variation of optical spectra in PM-HN-DSF when the fiber input power is changed from 3 to 25 mW. The fiber length is 100 m.

Using very low birefringent fiber, Islam *et al.* observed the soliton trapping between the two orthogonal polarization components [21]. In this study, we have not observed the phenomenon of soliton trapping. When the polarization direction of the PM fiber is inclined from the birefringent axis, the two-colored soliton pulses are simultaneously generated [8]. If the magnitude of birefringence of the PM fiber is much smaller to be $\sim 10^{-5}$, the phenomenon of soliton trapping may occur between the orthogonal polarization components.

IV. Supercontinuum Generation Using Highly Nonlinear Fiber

Using the dispersion-shifted fibers, we can generate the wavelength-tunable soliton pulse and anti-stokes pulse [10]. These two pulses shift toward the opposite wavelength sides as the fiber input power is varied. Using these two pulses, we can obtain the wavelength-tunable ultrashort pulses in the wavelength region of 1.3–1.76 μm.

The wavelength shift of the wavelength-tunable soliton pulse is induced by the nonlinear effect in the optical fibers. Thus it is considered that if the nonlinearity of the fiber can be increased, we can obtain much wider wavelength shift.

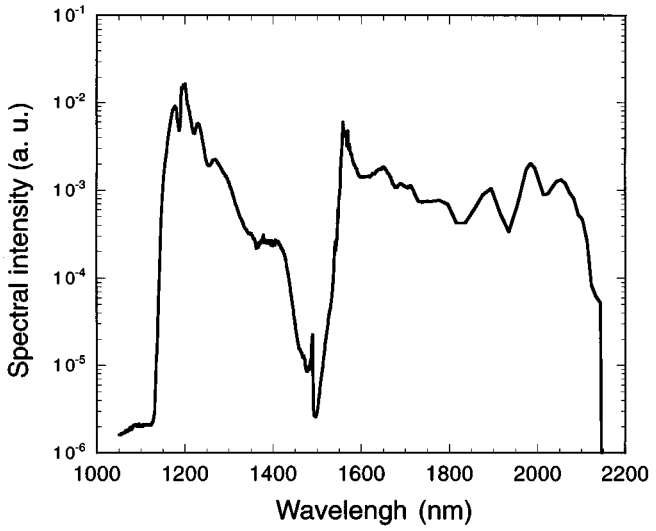

Fig. 9. Observed supercontinuum spectra generated in PM-HN-DSF. The fiber length is 100 m and the fiber input power is 25 mW.

In this section, we used the polarization maintaining highly nonlinear dispersion-shifted fibers (PM-HN-DSF) in order to get the wide wavelength tuning range [22]. In this fiber, the magnitude of $\beta_2 = -1.3$ ps^2/km and the mode-field diameter is 3.7 μm at the wavelength of 1.55 μm. The obtainable nonlinear coefficient γ is as large as 21 W^{-1}km^{-1}. This magnitude of the nonlinear coefficient is, to our best knowledge, the maximum one in the silica fibers [22]–[24].

Fig. 8 shows the variation of the optical spectra observed with the optical spectrum analyzer as the fiber input power is changed. The length of the fiber is 200 m. The wavelength region we can measure with the optical spectrum analyzer is from 600 to 1750 nm. When the fiber input power is 3 mW, the wavelength-tunable soliton pulse and anti-stokes pulse are generated at the longer and shorter wavelength sides of the pump pulse. The spectral shape of the generated soliton pulse is the clear sech^2 one. As the fiber input power is varied, the wavelengths of these pulses are also shifted continuously. Then as the fiber input power is increased, the soliton pulses and the corresponding anti-stokes pulses are generated one after another from the residual pump pulse. The spectra of these pulses are gradually overlapped, and finally, the widely broadened super continuum optical spectrum is constructed.

Fig. 9 shows the observed optical spectra on a log scale when the fiber input power is 25 mW. The optical spectrum is broadened from 1.1 to 2.1 μm. The 10-dB bandwidth is as broad as about 1 μm. To the best of our knowledge, the generation of the supercontinuum spectra is the first to reach a wavelength of 2 μm [19], [22], [25]–[29]. In this case, the peak power of the pump pulse is 4.7 kW and the pulse energy is only 520 pJ. When we use the 3-m-long fiber, the supercontinuum broadened from 1.2 to 1.9 μm is observed.

In Fig. 9, there is a deep dip around 1.5 μm. Several groups have been succeeded in the generation of a flat supercontinuum with a bandwidth of 200–300 nm using the dispersion-controlled fibers [22], [26], [27]. It is expected that much flatter continuum spectra can be obtained using the suitable fibers [30].

Recently, the supercontinuum generation broadened from 500 to 1600 nm has been demonstrated using the microstructure fiber [29]. If we use those special fibers, it is expected that the supercontinuum can be generated using the SHG pulse from the fiber laser.

The supercontinuum is useful for the ultrashort pulse generation, optical coherence tomography, etc. So far, it has been necessary to use the high pulse energy laser systems to generate the supercontinuum spectra. The system used in this experiment is very compact and almost maintenance free, and is very useful for practical applications.

V. Conclusion

Characteristics of the widely wavelength-tunable ultrashort pulse generation are experimentally analyzed for several types of PM fibers. Using the diameter-reduced type of polarization maintaining fibers, the wavelength-tunable soliton pulse is generated from 1.56 to 2.03 μm. The wavelength can be changed arbitrarily and continuously by varying the fiber input power. The SHG-FROG measurement of the soliton pulse around 2 μm is experimentally demonstrated for the first time. The almost transform-limited pedestal free 340-fs soliton pulse is observed.

Using the low-birefringent fibers, the orthogonally polarized small pulse spectrum is generated at the longer wavelength side of the soliton pulse when the polarization direction of the fiber input pulse is aligned along the slow axis. When the wavelength of the soliton is shifted toward the longer wavelength side by the soliton self-frequency shift, the orthogonally polarized small pulse spectrum is trapped by the soliton, and it is also shifted toward the longer wavelength side, keeping the wavelength separation. The effect of the birefringence is compensated by the chromatic dispersion.

Finally, a polarization maintaining dispersion-shifted highly nonlinear optical fiber is used as the sample fiber. When the fiber input power is not large, the wavelength-tunable soliton and anti-stokes pulses are generated. As the fiber input power is increased, the soliton and anti-stokes pulses are generated one after another, and the optical spectra are gradually overlapped each other. Thus the 1.1–2.1 μm widely broadened supercontinuum spectra are generated.

Acknowledgment

The authors would like to thank H. Nagai and M. Yoshida in AISIN SEIKI CO., Ltd for useful discussions and cooperation. They also thank M. Onishi, T. Okuno and M. Hirano, in Sumitomo Electric Industries, Ltd. for providing us with the PM-HN-DSF.

References

[1] I. N. Duling III, "Subpicosecond all-fiber erbium laser," *Electron. Lett.*, vol. 27, pp. 544–545, 1991.

[2] D. J. Richardson, R. I. Laming, D. N. Payne, M. W. Phillips, and V. J. Matsas, "320 fs soliton generation with passively mode-locked erbium fiber laser," *Electron. Lett.*, vol. 27, pp. 730–732, 1991.

[3] M. Nakazawa, E. Yoshida, and Y. Kimura, "Generation of 98 fs optical pulses directly from an erbium-doped fiber ring laser at 1.57 μm," *Electron. Lett.*, vol. 29, pp. 63–65, 1993.

[4] K. Tamura, E. P. Ippen, H. A. Haus, and L. E. Nelson, "77 fs pulse generation from a stretched-pulse mode-locked all-fiber ring laser," *Opt. Lett.*, vol. 18, pp. 1080–1082, 1993.

[5] W. H. Loh, D. Atkinson, P. R. Morkel, M. Hopkinson, A. Rivers, A. J. Seeds, and D. N. Payne, "All-solid-state subpicosecond passively mode-locked erbium-doped fiber laser," *Appl. Phys. Lett.*, vol. 63, pp. 4–6, 1993.

[6] M. E. Fermann, L.-M. Yang, M. L. Stock, and M. J. Andrejco, "Environmentally stable Kerr-type mode-locked erbium fiber laser producing 360 fs pulses," *Opt. Lett.*, vol. 19, pp. 43–45, 1994.

[7] N. Nishizawa and T. Goto, "Compact system of wavelength tunable femtosecond soliton pulse generation using optical fibers," *IEEE Photon. Technol. Lett.*, vol. 11, pp. 325–327, 1999.

[8] N. Nishizawa, R. Okamura, and T. Goto, "Simultaneous generation of wavelength tunable two-colored femtosecond soliton pulses using optical fibers," *IEEE Photon. Technol. Lett.*, vol. 11, pp. 421–423, 1999.

[9] ——, "Analysis of widely wavelength tunable femtosecond soliton pulse generation using optical fibers," *Jpn. J. Appl. Phys.*, vol. 38, pp. 4768–4771, 1999.

[10] ——, "Widely wavelength tunable ultrashort soliton pulse and anti-stokes pulse generation for wavelengths of 1.32–1.75 μm," *Jpn. J. Appl. Phys.*, vol. 39, pp. L409–L411, 2000.

[11] M. E. Fermann, A. Galvanaauskas, M. J. Stock, K. K. Wong, and D. Harter, "Ultrawide tunable Er soliton fiber laser amplified in Yb-doped fiber," *Opt. Lett.*, vol. 24, pp. 1428–1430, 1999.

[12] T. Hori, N. Nishizawa, H. Nagai, M. Yoshida, and T. Goto, "Electronically controlled high-speed wavelength-tunable femtosecond soliton pulse generation using acoustooptic modulator," *IEEE Photon. Technol. Lett.*, vol. 13, pp. 13–15, 2001.

[13] F. M. Mitschke and L. F. Mollenauer, "Discovery of the soliton self-frequency shift," *Opt. Lett.*, vol. 11, pp. 659–661, 1986.

[14] J. P. Gordon, "Theory of the soliton self-frequency shift," *Opt. Lett.*, vol. 11, pp. 662–664, 1986.

[15] B. Zysset, P. Beaud, and W. Hodel, "Generation of optical solitons in the wavelength region 1.37–1.49 μm," *Appl. Phys. Lett.*, vol. 50, pp. 1027–1029, 1987.

[16] P. Beaud, W. Hodel, B. Zysset, and H. P. Weber, "Ultrashort pulse propagation, pulse breakup, and fundamental soliton formation in a single-mode optical fiber," *IEEE J. Quantum Electron.*, vol. QE-23, pp. 1938–1946, 1987.

[17] Y. Matsuo, N. Nishizawa, M. Mori, and T. Goto, "Characteristics of wavelength tunable femtosecond soliton pulse generation using femtosecond pump laser and polarization maintaining fiber," *Opt. Rev.*, vol. 7, pp. 309–316, 2000.

[18] R. Trebino, K. W. DeLong, D. N. Fittinghoff, J. N. Sweetser, M. A. Krumbügel, B. A. Richman, and D. J. Kane, "Measuring ultrashort laser pulses in the time-frequency domain using frequency-resolved optical gating," *Rev. Sci. Instrum.*, vol. 68, pp. 3277–3294, 1997.

[19] G. P. Agrawal, *Nonlinear Fiber Optics*, 3rd ed. San Diego, CA: Academic, 2001.

[20] Y. Matsuo, N. Nishizawa, M. Mori, and T. Goto, "Measurement of timing jitter in wavelength tunable femtosecond soliton pulses," *Opt. Rev.*, vol. 7, pp. 317–322, 2000.

[21] M. N. Islam, C. D. Poole, and J. P. Gordon, "Soliton trapping in birefringent optical fibers," *Opt. Lett.*, vol. 14, pp. 1011–1013, 1989.

[22] T. Okuno, M. Onishi, T. Kashiwada, S. Ishikawa, and M. Nishimura, "Silica-based functional fibers with enhanced nonlinearity and their applications," *IEEE J. Select. Topics Quantum Electron.*, vol. 5, pp. 1385–1391, 1999.

[23] M. J. Holmes, D. L. Williams, and R. J. Manning, "Highly nonlinear optical fiber for all optical processing applications," *IEEE Photon. Technol. Lett.*, vol. 7, pp. 1045–1047, 1995.

[24] M. Onishi, T. Okuno, T. Kashiwada, S. Ishikawa, N. Akasaka, and M. Nishimura, "Highly nonlinear dispersion-shifted fibers and their application to broadband wavelength converter," *Opt. Fiber Technol.*, vol. 4, pp. 204–214, 1998.

[25] R. R. Alfano, *The Supercontinuum Laser Source*. New York: Springer-Verlag, 1989.

[26] T. Morioka, K. Mori, S. Kawanishi, and M. Saruwatari, "Pulse-width tunable, self-frequency conversion of short optical pulses over 200 nm based on supercontinuum generation," *Electron. Lett.*, vol. 30, pp. 1960–1962, 1994.

[27] Y. Takushima, F. Futami, and K. Kikuchi, "Generation of over 140-nm-wide super-continuum from a normal dispersion fiber by using a mode-locked semiconductor laser source," *IEEE Photon. Technol. Lett.*, vol. 10, pp. 1560–1562, 1998.

[28] C. X. Yu, H. A. Haus, E. P. Ippen, W. S. Wong, and A. Sysoliatin, "Gigahertz-repetition-rate mode-locked fiber laser for continuum generation," *Opt. Lett.*, vol. 25, pp. 1418–1420, 2000.
[29] J. K. Ranka, R. S. Windeler, and A. J. Stentz, "Visible continuum generation in air-silica microstructure optical fibers with anomalous dispersion at 800 nm," *Opt. Lett.*, vol. 25, pp. 25–27, 2000.
[30] N. Nishizawa and T. Goto, "Widely broadened super continuum generation using highly nonlinear dispersion shifted fibers and femtosecond fiber laser," *Jpn. J. Appl. Phys.*, vol. 40, pp. L365–L367, 2001.

Norihiko Nishizawa (M'99) was born in Sendai, Japan, on January 5, 1969. He received the M.E. and Ph.D. degrees in quantum engineering from Nagoya University, Nagoya, Japan, in 1993 and 1995, respectively.

Since 1995, he has been an Assistant Professor in the Department of Quantum Engineering, Nagoya University. His research fields are ultrafast nonlinear optics, quantum optics, and optical communication in next generation.

Dr. Nishizawa is a member of the Japan Society of Applied Physics, the Institute of Electronics, Information, and Communication Engineers of Japan, the Laser Society of Japan, and OSA.

Toshio Goto (SM'92) was born on November 11, 1941. He received the B.E, M.S., and Ph.D. degrees in electronic engineering from Nagoya University, Nagoya, Japan, in 1964, 1966, and 1969, respectively.

In 1969, he became a Research Associate and in 1986 a Professor at Nagoya University. Since 2000, he has been the Dean of Graduate School of Engineering at Nagoya University. His main fields of interest are application of lasers in materials engineering and microelectronics, gaseous electronics, and application of lasers in quantum optics. Since 2000, he has been Vice-President of the Japan Society of Applied Physics.

Dr. Goto is a member of the Institute of Electrical Engineers of Japan, the Institute of Electronics, Information, and Communication Engineers of Japan, and the Laser Society of Japan.